

---

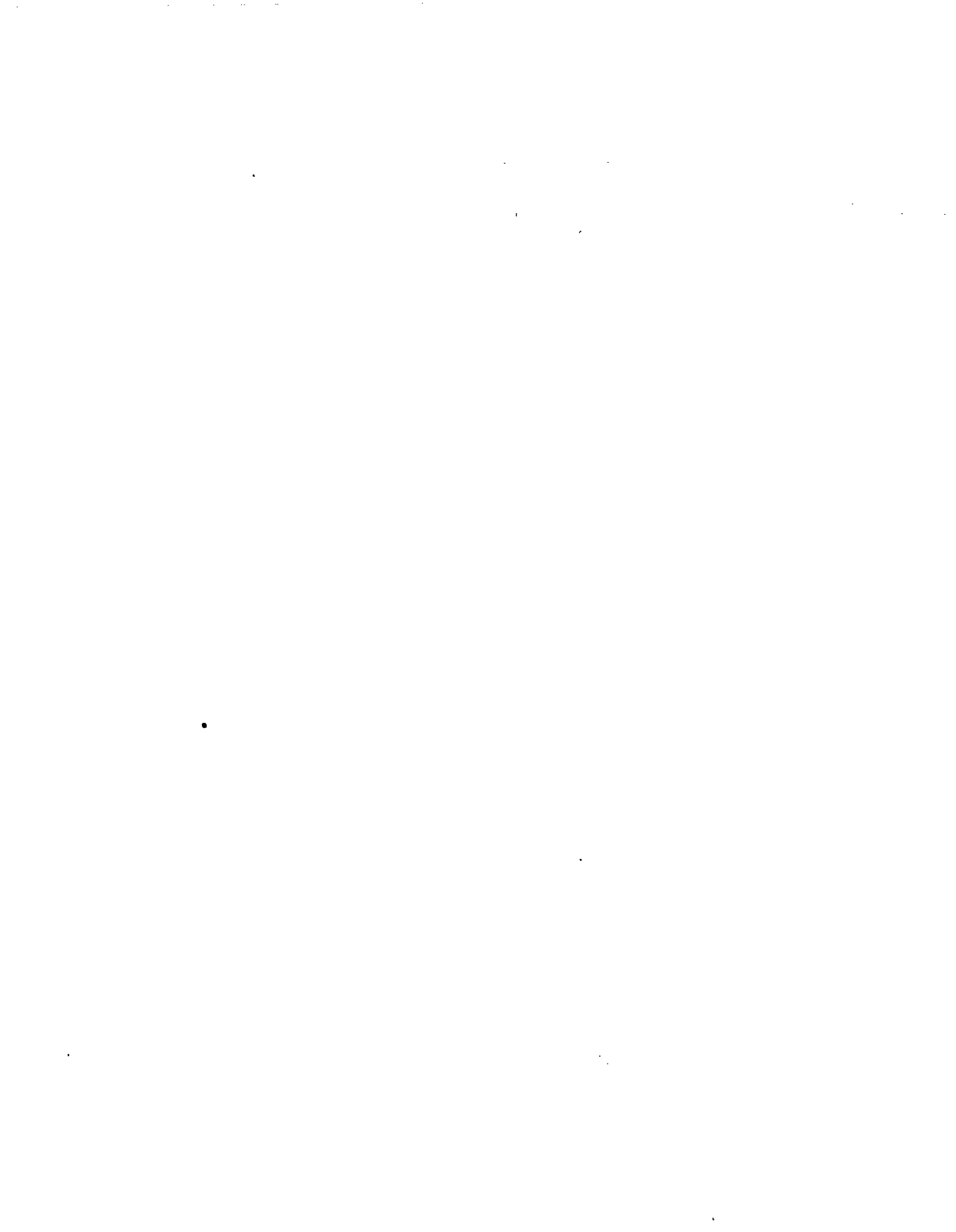
---

**REPORT No. 311**

---

**AERODYNAMIC THEORY AND TEST OF STRUT FORMS**

**By R. H. SMITH**  
**Aerodynamical Laboratory, Bureau of Construction**  
**and Repair, U. S. Navy**



# REPORT No. 311

## AERODYNAMIC THEORY AND TEST OF STRUT FORMS

By R. H. SMITH

### PART I<sup>1</sup>

#### SUMMARY

*This report, submitted to the National Advisory Committee for Aeronautics for publication, presents the whole study under this title in two parts, only the first of which is reported here. In this part the symmetrical inviscid flow about an empirical strut of high service merit is found by both the Rankine and the Joukowski methods. The results can be made to agree as closely as wished. Theoretical stream surfaces as well as surfaces of constant speed and pressure in the fluid about the strut are found. The surface pressure computed from the two theories agrees well with the measured pressure on the fore part of the model but not so well on the after part. From the theoretical flow speed the surface friction is computed by an empirical formula. The drag integrated from the friction and measured pressure closely equals the whole measured drag. As the pressure drag and the whole drag are accurately determined, the friction formula also appears trustworthy for such fair shapes.*

#### INTRODUCTION

The mathematical treatment of symmetrical flow past symmetrical bodies, which are streamlined for low resistance, is directed toward the solution of one of two general problems. Either one seeks to determine the nonviscous flow past forms whose rooting<sup>2</sup> is specified but final shape unknown, or about those whose final shape is specified and rooting unknown. The latter, being the inversion of the other, may be called the inverse problem, while the former may be called the direct problem. Almost all of the theoretical investigation on fluid flow past such shapes has been devoted to forms of fixed rooting, although they are, technically at least, the less important of the two. This partiality to the direct problem results from the fact that it naturally runs along with, while the other runs counter to, a mathematical development which is practically irreversible; that is, one which can be followed in the reverse direction only with the greatest difficulty.

Following logically the theory of fluid motion, the direct problem was successfully studied early, in the case of poorer forms of simple origin, in both two and three dimensions. The method was that due to Rankine, in which sources and sinks of equal total strength are imagined created along a streamline of a uniform stream of fluid, and the separate streams, each flowing as if alone, combined by superposition. (References 1, 2, and 3.) The closed surface of separation between the source-sink and the external streams is then made the surface of a solid body. The substitution of this body for the source-sink flow leaves the external stream unchanged since (in a nonviscous fluid) the inner flow and the body produce the same boundary conditions at the surface of separation. Since the external stream is known from the superposition of the flows before the substitution, the flow about the body is known.

Such surfaces of separation for water, suitable as forms for surface ships, have since been derived graphically by Taylor (References 3 and 4) and McEntee (Reference 5) by assuming more complicated source-sink combinations. These forms are made long and narrow with

<sup>1</sup> This part was submitted in May, 1928, to the Johns Hopkins University in conformity with the requirements for the M. A. degree. The second part will be completed and the whole submitted in 1929 in conformity with the requirements for the Ph. D. degree.

<sup>2</sup> By rooting is meant the premises which fix the form of the body, namely, the arrangement of the sources and sinks in the Rankine theory or of the complex poles in the Joukowski theory.

sharp, or sharply rounded, bows and sterns, in order to reduce the wave-making and inertia forces which together are large compared to the viscous forces. Because of their large surfaces such forms are not suited, however, for deep submersion in either water or air, where the viscous forces predominate.

While the development of deep-sea shapes of least drag has been very little studied because of their lack of utility, the practical need for minimum resistance air forms has led to a large amount of experimentation on empirical and, to a much less extent, on theoretical streamline forms. An important experiment on theoretical airship forms was made by G. Fuhrmann in 1912. (Reference 6.) Using Taylor's graphical method, he derived six beautifully streamlined separation surfaces of revolution, and showed the agreement between the surface pressures about them as computed and as experimentally measured. The 2-dimensional sequel to Fuhrmann's work is the subject of Part II of this general study, and was suggested to me by Dr. A. F. Zahm as suitable for a thesis.

In two dimensions, the direct problem can be treated also by the method of conformal transformation. An extensive literature has been built up during the last few years on the development of Joukowski and kindred airfoils by this method. (References 7, 8, 9, 10, 11, and 12.) The corresponding development of symmetrical shapes suitable for struts, however, has been little studied although the strut derivatives of Joukowski profiles are more easily obtained and are more like successful service forms. A Joukowski strut of high merit is developed in the present study, and the theoretical and experimental flows about it are compared.

The inverse problem, in which the final shape is specified, has been undertaken in only one investigation. (Reference 14.) Von Karman found the flow past arbitrary half bodies of revolution, and then past an airship, whose shape was specified, by forming its bow and stern of two half bodies, cut to the correct length, and joining them. Certain approximations and assumptions incident to the splicing were made and investigated. While they shorten a very long problem until it is practically solvable, these approximations destroy much of the mathematical elegance and exactness of the method.

Since Von Karman's method is an important theoretical and technical advance, it has been thought worth while to carry through, at least once, the laborious task of extending it rigorously to an arbitrary whole body. The body chosen was the United States Navy Number 2 strut, whose form is empirical and whose service merit (Reference 13) is unexcelled. This investigation, together with that of the Joukowski strut referred to, which differs from the Navy Number 2 only at the extreme trailing edge, gives two independent developments of the theoretical flow about this strut. The two theoretical flows are finally compared with the experimental flow found by measuring the pressure over the strut surfaces. The Von Karman and Joukowski strut studies constitute Part I of the whole investigation.

Whether we consider the problem of solving the flow about a strut of fixed final form or of fixed rooting, the mathematical treatment is possible only when viscosity is neglected. Under usual conditions, it is well established that fluids, like air and water, stick without slipping to the surface of the body past which they flow, and that the retardation of the near-by fluid takes place in a thin layer called the boundary layer. In this layer the viscous forces are of the same order of magnitude as the inertia forces and lead to the formation of vortices when the retardation is sufficient to cause a reverse flow. (References 15 and 16.) Such sufficient retardations always occur in the immediate wake of conventional streamline bodies, particularly if their trailing parts are blunt. The surface line dividing the upstream region of nonreverse flow and the downstream region of reverse flow, is called the line of separation. The shifting of this line with change of air speed, in the case of some forms, is one cause for the variation of the resistance coefficient with Reynolds Number. The line of separation for easy shapes is never far from the aftmost point of the body and shifts most for those with rounded tails. For well streamlined bodies with sharp tails or trailing edges, the line of separation is sometimes stationary for a considerable range of Reynolds Number. Such forms produce a stable flow whose pattern is fixed and have a very low resistance, most of which is found to be due to viscous friction. They represent the optimum easy forms and are the most interesting from

the practical, as well as from the theoretical, point of view. The struts considered here are bodies of this class.

THE SOURCE-SINK ENVELOPE APPROXIMATING THE UNITED STATES NAVY NUMBER 2 STRUT

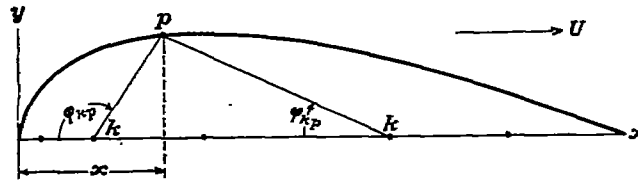


FIGURE 1

At any point  $p$  on the separation line (fig. 1) inclosing a source-sink system in a plane stream  $U$ , clearly the stream function is

$$\psi_p = 0 = Uy - \sum \frac{\varphi_{kp} Q}{2\pi} \tag{1}$$

where  $Q$  is the strength of any source or sink and  $\varphi_{kp}$  the angle as shown. The condition of closure, viz, that the  $Q$  flow shall stay inside the line, is

$$\sum Q = 0 \tag{2}$$

Hence, if  $y, \varphi$  are given for enough points  $p$ , equations (1), (2) determine the  $Q$ 's that condition the given closure line in the given stream. Let the closure line be the section of the United States Navy Number 2 strut in the plane stream  $U$ .

Equation (1) is true, in two dimensions, for any type or distribution of sources and sinks. It will be convenient to assume line sources and sinks which run in the strut plane of symmetry parallel to the strut length, and located on the ordinates by which the strut is specified. There will then be  $n$  sources and sinks and  $n$  equations of type (1), for  $n$  ordinates. To meet the condition of closure, equation (2) is added and another source or sink, making in all  $n+1$  sources and sinks and  $n+1$  equations.

Since its curvature is important, a streamline form can not be specified by fewer than 10 or 12 ordinates judiciously chosen. In this study, 12 coordinates are used to fix the form, and one coordinate added at the stern to fix the position of the thirteenth source or sink. The coordinates for the United States Navy Number 2 strut, multiplied by 2, (fig. 2) are as follows:

$p$	$x$	$y$	$p$	$x$	$y$	$p$	$x$	$y$
0	0	0	5	2.600	2.360	10	16.800	1.700
1	.200	.680	6	4.200	2.751	11	18.400	1.202
2	.600	1.200	7	7.200	3.000	12	20.000	.570
3	1.000	1.551	8	10.400	2.920	13	20.500	.290
4	1.600	1.918	9	13.600	2.418	14	21.000	0

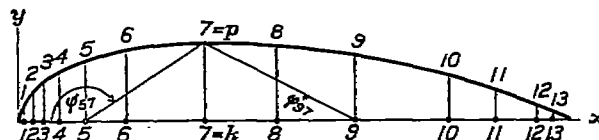


FIGURE 2

Hence, the value of  $\varphi_{57}$ , for example, is  $\varphi_{57} = \pi - \tan^{-1} \frac{3.000}{7.20 - 2.60} = \pi - 0.578 = +2.564$ . Likewise the value of  $\varphi_{77}$  is found to be  $\varphi_{77} = \tan^{-1} \frac{3.000}{13.60 - 7.20} = +0.438$ . After substituting the numerical values for the coefficients and unity for the value of  $U$ , the constants of equations (1) and (2) take the form given in Table I.

There is nothing new, and very little of interest, in the way this system of linear equations has been solved. The solution was accomplished in steps, each of which reduced the number

both of equations and of unknowns by one. After each reduction the new equations were rearranged so that the next reduction could be made by using factors of the order of unity. For example, the first reduction was made by eliminating column 2, Table I, by multiplying the second row by  $-0.9624$ , and adding the result to the first row, then by multiplying the third row by  $-0.6614$  and adding to the second row, and so on down the column. The new set, so obtained, contains no  $Q_2$  column, and has only 12 rows. These rows were rearranged for the next reduction in the order 1, 12, 10, 8, 7, 5, 3, 2, 4, 6, 9, 11, and multiplied, as before, by the proper factors to eliminate column 7. Carrying through this process to the end involves almost prohibitive work. Ways to save labor and chance of error by proper tabulation are obvious, however, and success depends principally on how well they are used. Numbers of seven places or more must be carried throughout, which increases considerably the chance of error. Table I is given here reduced from seven places to four places for brevity. The solution of this set of 13 equations was found to be

$$\begin{array}{lll} Q_1 = + 1.6650 & Q_5 = + 7.0304 & Q_9 = - 3.3078 \\ Q_2 = - 5.8767 & Q_6 = - 2.1855 & Q_{10} = - .1097 \\ Q_3 = + 13.0072 & Q_7 = + .8824 & Q_{11} = - 3.2608 \\ Q_4 = - 5.8817 & Q_8 = - 1.2550 & Q_{12} = + 1.0123 \\ & & Q_{13} = - 1.7202 \end{array}$$

Figure 3 shows graphically the distribution and the relative strengths of the sources and sinks along the chord of the strut profile. A positive  $Q$  is a source, a negative one a sink, by defini-

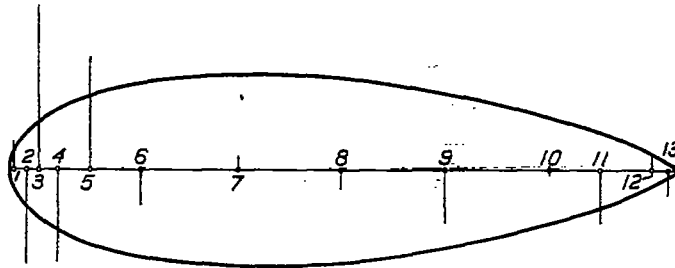


FIGURE 3.—The distribution and relative strengths of sources and sinks whose separation surface in a unit stream is indistinguishable from the United States Navy No. 2 strut

tion, hence there are five sources and eight sinks, the sources predominating at the bow and the sinks at the stern.

It is relatively easy to find the components of velocity and the pressure at each surface point  $p$ , from the known strengths and positions of the sources and sinks. The stream function  $\psi_{kp}$ , at each point  $p$ , due to the  $k^{\text{th}}$  source or sink, is simply

$$\psi_{kp} = \frac{Q_k}{2\pi} \varphi_{kp}$$

and the radial velocity  $q_{kp}$ , simply

$$q_{kp} = \frac{\partial \psi_{kp}}{\partial \varphi_{kp}} = \frac{Q_k}{2\pi r_{kp}}$$

where  $r_{kp} = [(x_p - x_k)^2 + y_p^2]^{1/2}$ . The cartesian components of  $q_{kp}$  are

$$u_{kp} = \frac{Q_k(x_p - x_k)}{2\pi r_{kp}^2}, \quad v_{kp} = \frac{Q_k y_p}{2\pi r_{kp}^2},$$

which become, when summed for all sources and sinks,

$$u_p = \frac{1}{2\pi} \sum_1^{13} \frac{Q_k(x_p - x_k)}{r_{kp}^2} \quad (3)$$

$$v_p = \frac{1}{2\pi} \sum_1^{13} \frac{Q_k y_p}{r_{kp}^2} \quad (4)$$

The velocity  $U_0$  of the uniform stream must be added to  $u_p$ , giving

$$q_p = [(U_0 + u_p)^2 + v_p^2]^{1/2} \tag{5}$$

for the resultant velocity of  $p$ . Then the pressure  $p_p$  at  $p$ , above the stream pressure, is

$$p_p = p_0 \left( 1 - \frac{q_p^2}{U_0^2} \right) \tag{6}$$

where  $p_0$  is the dynamic pressure,  $\frac{1}{2} \rho U_0^2$ , of the distant stream and  $p_p$  is in terms of  $p_0$  as a unit.

Table II gives the values of  $u_p$ ,  $v_p$ ,  $q_p$ , and  $p_p$  derived from equations (3), (4), (5), and (6) for the United States Navy Number 2 strut. The values of the point pressure  $p_p$  are shown plotted against the strut width in Figure 4 and against its half thickness in Figure 5. The

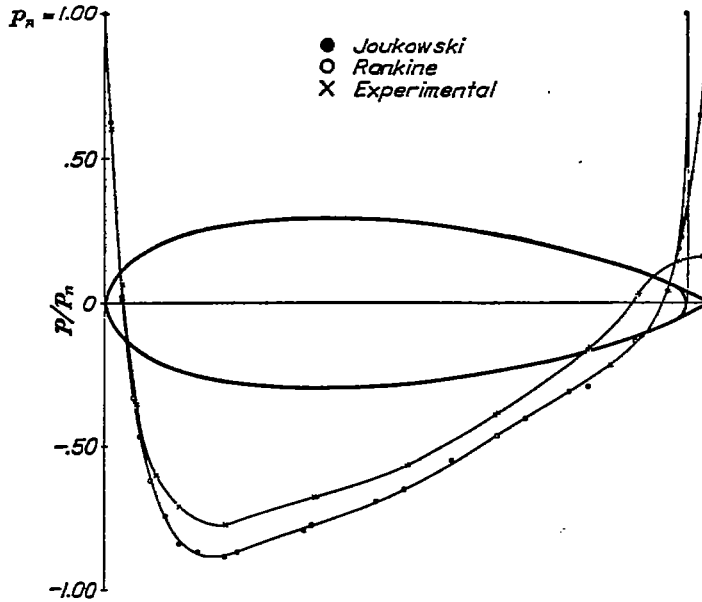


FIGURE 4.—Curves of point pressure,  $p/p_0$ , over surface of Navy No. 2 strut from experiment and from Rankine and Joukowski theories

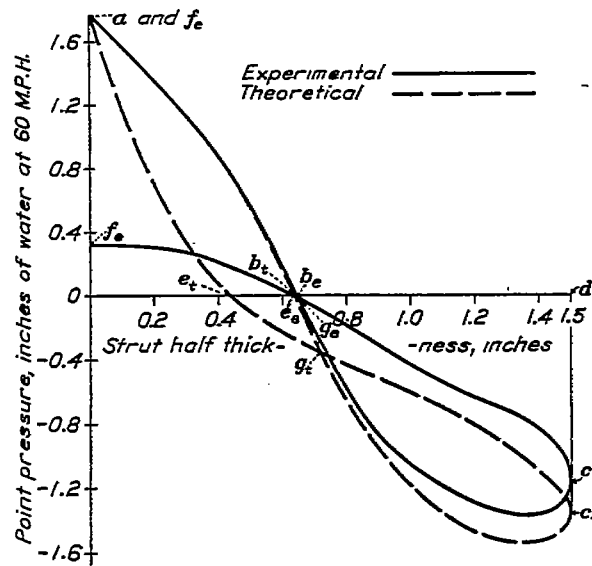


FIGURE 5.—Point pressure versus strut half thickness for experiment and theory. The Joukowski and Rankine theoretical curves coincide

integrated pressural drag is clearly proportional to the difference between the areas  $a b g e f$  and  $g c g$  of the theoretical curve (fig. 5), which is found to be zero when the two areas are planimeted. The theoretical resistance of this empirical strut is, therefore, zero. Figures 4 and 5 also give the point pressures found by measurement and by the Joukowski theory, which will be explained presently.

The calculation of the streamlines and velocity distribution afield would be long, but not difficult, by use of equations (3) to (6). They are more easily found when the strut is considered as a Joukowski profile. These extensions of the development of the flow about the strut will, therefore, be left for the Joukowski treatment, now to be considered.

#### THE JOUKOWSKI STRUT WHOSE FORM APPROXIMATES THE UNITED STATES NAVY NO. 2

The method of finding wing and other streamline forms by a conformal transformation of circular and elliptic cylinders is due to Joukowski and later to Mises, Betz, Muller, Witoszynski, and others. (References 7, 8, 9, 10, 11, 12.) Strictly speaking, the Joukowski profiles are those of simple 2-pole origin with upper and lower lines forming a cusp at the trailing edge. These profiles were soon extended by his followers, in an effort to derive more practical wings, to forms of multi-pole origin and to those whose upper and lower surfaces intersect at a small angle at the trailing edge.

The general theory of conformal transformation of plane flow has been well worked out in the wing studies cited, and will not be considered here, except to mention two theorems. The law of Riemann, in the theory of functions, states that there is a circle and surrounding potential field into which one can transform any simple holomorphic contour and surrounding potential field so that the field at infinity remains unchanged. Then, more recently, the theorem of Bieberbach, which states that there is one, and only one, function for this transformation, namely,

$$\zeta = z + \frac{a_1}{z} + \frac{a_2}{z^2} + \frac{a_3}{z^3} + \dots \quad (7)$$

in which  $\zeta = \xi + i\eta$  are the coordinates in the  $\zeta$  plane of the circle and  $z = x + iy$  are the coordinates in the  $z$  plane of the contour. These theorems apply, naturally, only in two dimensions.

Equation (7) may be written

$$\frac{d\zeta}{dz} = \left(1 - \frac{c_1}{z}\right) \left(1 - \frac{c_2}{z}\right) \left(1 - \frac{c_3}{z}\right) \left(1 - \frac{c_4}{z}\right) \dots \quad (8)$$

where  $c_n$  are the complex poles of the transformation, and  $\sum c_n = 0$ . The Joukowski solution of the inverse problem, viz, of transforming a circle and flow field to a given profile with corresponding field, reduces to the task of finding the  $c_n$  or the  $a_n$  complex coefficients in these equations. The direct problem, on the other hand, begins with these given in the premises, and has been studied, with some difficulty, up to five poles. (Reference 11.) It would be surprising if fewer than this number were sufficient to fix satisfactorily the transformation of a circle to an arbitrary streamline form. The theory in its present state gives no practical way to determine even five poles which would produce roughly a specified form. The Joukowski method, therefore, gives no solution yet of the inverse problem. One must resort to a fit and try method to find a Joukowski strut that coincides with one arbitrarily chosen and be satisfied with a good approximation. This method will be used to find the Joukowski strut that approximates the United States Navy Number 2.

In carrying out this approximation a modified Joukowski profile will be used, but before considering the profile it may be well to summarize briefly that part of the Joukowski theory which applies to symmetrical flow. The theory begins with the very old transformation by which a circle of radius  $b$  is flattened into a straight line whose length is  $4b$ . The transformation formula is the simple 2-pole equation

$$z = \zeta + \frac{b^2}{\zeta} \quad (9)$$

which decomposes into two equations,

$$\begin{aligned} x &= \xi \left( 1 + \frac{b^2}{\xi^2 + \eta^2} \right) \\ y &= \eta \left( 1 - \frac{b^2}{\xi^2 + \eta^2} \right) \end{aligned} \tag{10}$$

The same transformation flattens circles, concentric with the map circle  $r=b$ , into ellipses and distorts their radii into hyperbolas, the ellipses and hyperbolas being focused at the ends of the line  $4b$ , Figure 6.

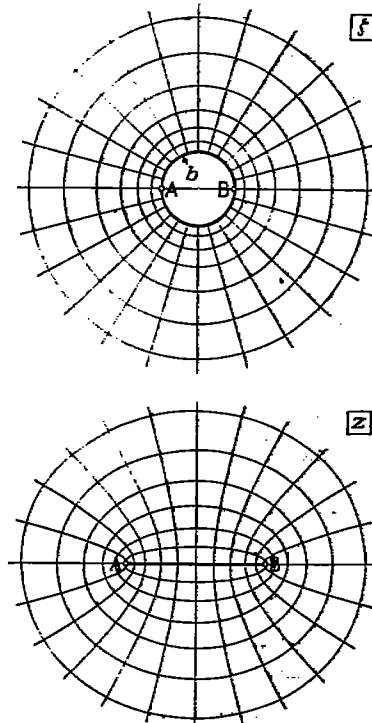


FIGURE 6.—Conformal transformation of map circle,  $r=b$ , and its potential field into the straight line  $4b$  and its potential field

For a uniform stream crossing a solid cylinder  $r=b$ , the streamlines,  $\psi_r = \text{const.}$  graded from the circle  $r=b$ , in the  $\zeta$  plane, become transformed into straight parallel lines graded from the line  $4b$  in the  $z$  plane, and the curves  $\varphi_r = \text{const.}$  become straight lines orthogonal to them, the two sets of lines forming together an ordinary cartesian network. The said flow about the circular cylinder  $r=b$ , is thus transformed into the flow past a flat plane lying along the general stream.

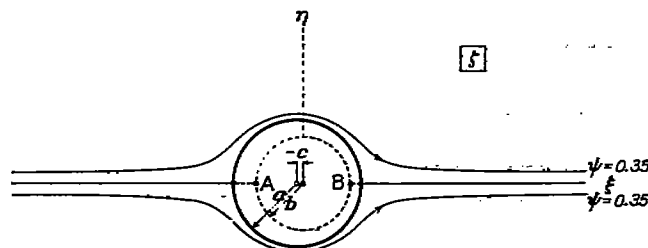


FIGURE 7a.—Round cylinder,  $a=2.00$ , centered at  $c=-0.20$  map cylinder,  $b=1.48$ , transformed into Joukowski approximation of United States Navy No. 2 strut, Figure 7b

Similarly, for flow across the solid cylinder  $a > b$ , the curves  $\psi_r = \text{const.}$  graded from the concentric circle  $r=a > b$ , in the  $\zeta$  plane, become curves  $\psi_z = \text{const.}$  graded from the corresponding ellipse in the  $z$  plane. The flow about the circular cylinder  $r=a$  is transformed, in this way, into the flow about an elliptic cylinder, focused at  $x = \pm 2b$ . When the circle  $r=a$  is not concentric with the map circle,  $r=b$ , but eccentrically centered at  $\xi = -c$  (fig. 7a), the curve in the

$z$  plane corresponding to  $r=a$ , becomes an ellipse distorted into a more or less streamline strut form. (Fig. 7b.) If the shift of the circle  $r=a$  along  $-\xi$  is sufficient to make  $c=b-a$ —that is, to make the circles tangent at  $\xi=b$ —the trailing edge of the strut degenerates to a cusp, and one has a symmetrical Joukowski profile.

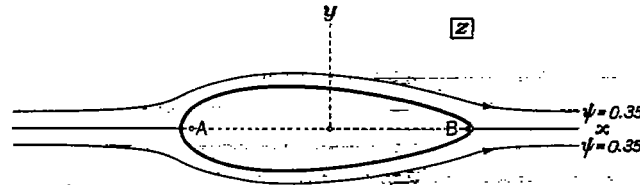


FIGURE 7b.—Joukowski approximation of endless United States Navy No. 2 strut, transformed from endless round cylinder, Figure 7a

By trying a number of sizes and positions for the circle  $r=b$ , one finds without much difficulty that the map circle  $b=1.48$ , transforms the circle  $a=2.00$ , centered at  $\xi=-0.20$  into the Navy Number 2 strut accurately to within  $1\frac{1}{2}$  per cent of the maximum ordinate everywhere except near the extreme trailing edge. The actual agreement is seen in Table III and Figure 8.

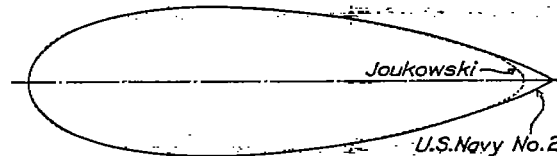


FIGURE 8.—Joukowski approximation to United States Navy No. 2 strut

This agreement is satisfactory, especially since most, if not all, of the objectionable discrepancy near the trailing edge, where the Joukowski strut is rounded while the Navy Number 2 continues to an edge, occurs aft the lines of separation where the form of the surface is largely immaterial.

Having obtained the Joukowski strut, the flow about it is easily found. In general, the flow about a circular cylinder of radius  $a$  is given by the equation

$$\phi_r + i\psi_r = U_0 \left( \zeta + \frac{a^2}{\zeta} \right) \quad (11)$$

whose  $\psi_r$  component is

$$\psi_r = U_0 \eta - \frac{U_0 \eta a^2}{\xi^2 + \eta^2} \quad (12)$$

When the cylinder is centered at  $\xi = -0.20$ , and has a radius  $r = a = 2.00$ , equation (12) becomes

$$\psi_r = U_0 \eta - \frac{4 U_0 \eta}{\eta^2 + (\xi + 0.20)^2}, \quad (13)$$

whence the component velocities at any point  $(\xi, \eta)$  about the cylinder are

$$u_r = \frac{\partial \psi_r}{\partial \eta} = U_0 \left\{ 1 - 4 \frac{(\xi + 0.20)^2 - \eta^2}{[(\xi + 0.20)^2 + \eta^2]^2} \right\} \quad (14)$$

$$v_r = -\frac{\partial \psi_r}{\partial \xi} = 8 U_0 \eta \frac{\xi + 0.20}{[(\xi + 0.20)^2 + \eta^2]^2} \quad (15)$$

In order to find the corresponding components  $u_z$  and  $v_z$  about the strut, the lengths of corresponding path segments in the  $\zeta$  and  $z$  planes must be found. That is, the differential quotient of  $z$  and  $\zeta$  must be evaluated. Then

$$\frac{u_r}{u_z} = \frac{v_r}{v_z} = \left| \frac{dz}{d\zeta} \right| \quad (16)$$

The evaluation of  $\left|\frac{dz}{d\xi}\right|$  is known, and can be easily varied to be

$$\left|\frac{dz}{d\xi}\right| = \frac{1}{\xi^2 + \eta^2} \{(\xi^2 + \eta^2 - b^2)^2 + 4b^2\eta^2\}^{1/2} \quad (17)$$

Finally, the resultant velocity  $q_r$ , at any point  $\zeta$ , about the cylinder is given by

$$q_r^2 = u_r^2 + v_r^2 \quad (18)$$

Likewise the resultant velocity  $q_s$ , at any point,  $z$ , about the strut is given by

$$q_s^2 = u_s^2 + v_s^2 \quad (19)$$

The surfaces of constant speed or pressure near the cylinder are easily found analytically, but those near the strut can not easily be found directly.<sup>3</sup> In the latter case, the values of  $q_s$  must be found along a number of closely graded streamlines, and the surfaces of constant  $q_s$  found by use of an auxiliary plot of  $q_s$  for each streamline, first against  $x$  and then against  $y$ .

The surfaces of constant speed  $q_r$ , about the cylinder (References (18) and (21)) may be found as follows. If the velocity  $U_0$  of the uniform stream is unity, equation (12), in polar coordinates, takes the form

$$\psi_r = \left(r - \frac{a^2}{r}\right) \sin \theta \quad (20)$$

By differentiation, equation (20) gives the two polar components of velocity,

$$\left. \begin{aligned} q_r &= \frac{\partial \psi_r}{\partial r} = \left(1 + \frac{a^2}{r^2}\right) \sin \theta \\ q_\theta &= \frac{\partial \psi_r}{r \partial \theta} = \left(1 - \frac{a^2}{r^2}\right) \cos \theta \end{aligned} \right\} \quad (21)$$

Hence

$$q_r^2 = q_r^2 + q_\theta^2 = \left(1 + \frac{a^2}{r^2}\right)^2 \sin^2 \theta + \left(1 - \frac{a^2}{r^2}\right)^2 \cos^2 \theta$$

or

$$q_r = \frac{1}{r^2} [(a^2 + r^2)^2 - 4a^2 r^2 \cos^2 \theta]^{1/2} \quad (22)$$

From this equation  $q_r$  clearly has the maximum value 2, at the point where  $\theta = \frac{\pi}{2}$  and  $r = a$ , and the minimum value, zero, at the rest points  $\theta = 0, \pi, r = a$ . Surfaces of constant speed  $q_r$ , intermediate between 0 and 2 are shown, plotted from Table IV, in Figure 9a, where those above the  $\xi$  axis are for even speeds, those below for even pressures.

One surface of constant speed is of special interest—namely, the surface  $q_r = 1$ —showing where the speed beyond the cylinder is equal to that of the uniform stream. For this case

$$r^4 = (a^2 + r^2)^2 - 4a^2 r^2 \cos^2 \theta \quad (23)$$

or

$$a^2 + 2r^2 (1 - 2 \cos^2 \theta) = 0.$$

Since  $\cos^2 \theta = \frac{\xi^2}{\xi^2 + \eta^2}$ , equation (23) becomes

$$a^2 + 2(\eta^2 - \xi^2) = 0,$$

from which

$$\frac{\xi^2}{K} - \frac{\eta^2}{K} = 1, \text{ where } K = \frac{a^2}{2}. \quad (24)$$

<sup>3</sup> Surfaces of constant speed and pressure are of practical interest in showing where to place anemometers to indicate, with least correction, the relative speed of the strut and the general air stream.

The surfaces  $q_t = U_0$  are therefore two equilateral hyperbolas with foci at the ends of the cylinder diameter which lies along the general stream. (Fig. 9a.)

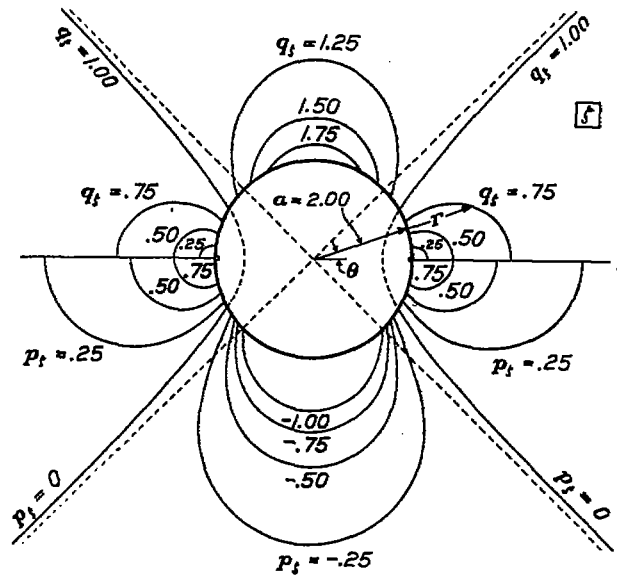


FIGURE 9a.—Lines of constant speed and pressure of perfect flow past endless round cylinder

To find the corresponding surfaces of constant speed near the strut, one must first determine a number of closely graded streamlines near the cylinder, and the corresponding ones about the strut. Equation (13) must, therefore, be solved for a number of values of  $\psi_t$  and the values  $\xi$  and  $\eta$  transformed to  $x$  and  $y$  by equation (10). Since  $\psi_t$  is a cubic in  $\eta$  and only a quadratic in  $\xi$ , equation (13) is best put in the form,

$$\xi + 0.20 = \eta \left[ \frac{1 - \frac{\psi_t}{\eta} - \left(\frac{a}{\eta}\right)^2}{\frac{\psi_t}{\eta} - 1} \right]^{1/2} \tag{25}$$

and solved for  $\xi$ . The values  $\xi, \eta, x, y$  of the streamlines useful in finding surfaces of constant speed about the strut, as well as values of  $\left| \frac{dz}{dz_t} \right|$  and the velocities  $q_t$  and  $q_s$ , are illustrated in Table V-b, which is for the streamline  $\psi_t = 0.01$  only. The coordinates of the constant speed curves taken, as explained, from auxiliary plots of speed versus  $x$  and  $y$  for each streamline are given in Table VI, for as many of the even speeds and pressures, used for the cylinder, as exist for the strut. Since the maximum speed about the strut, Table Va, is  $q_s = 1.37$ , and the minimum pressure  $p_s = -0.867$ , the curves  $q_s = 1.5, 1.75$  and  $p_s = -1.00$ , given for the cylinder, do not appear for the strut. The curves for constant  $q_s$  intermediate between 0 and 1.37 are

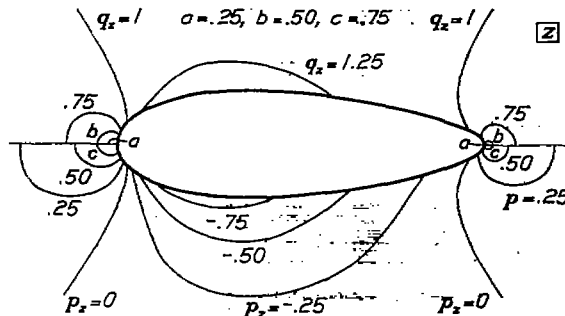


FIGURE 9b.—Lines of constant speed and pressure for perfect flow past United States Navy No. 2 strut (Joukowski approximation) at zero pitch and yaw

shown in Figure 9b, where again those above the  $x$  axis are for even speeds, and those below are for even pressures.

The computed point pressures over the surface of the Joukowski strut are given in Table Va, and plotted against strut width in Figure 4, along with the computed pressures for the Rankine strut and those measured by experiment. The plot of pressure against strut half-thickness (fig. 5) coincides with that for the Rankine strut. Hence the theoretical resistance of the Joukowski strut is zero also.

Normally graded streamlines,  $\psi = \text{const.}$ , are found about the round cylinder, and then transformed to those about the strut, by the equations already used to find the surfaces of constant speed. The values computed for these curves are illustrated in Table Vc, which is for the streamline  $\psi = 0.35$  only. A number of evenly graded streamlines are drawn past both the round cylinder and the strut in Figures 10a and 10b.

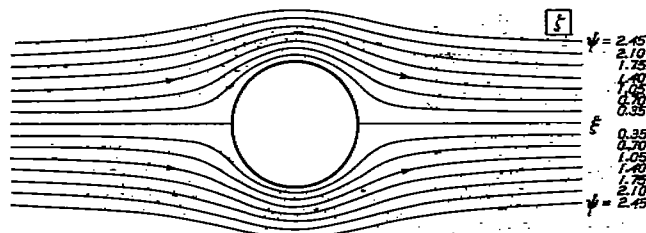


FIGURE 10a.—Round cylinder fixed in a boundless uniform stream of inviscid fluid

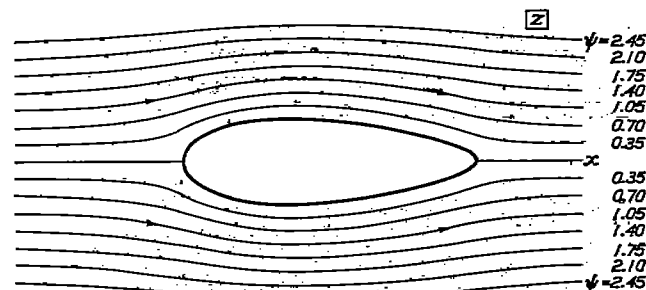


FIGURE 10b.—United States Navy No. 2 strut (Joukowski approximation) fixed in a boundless uniform stream of inviscid fluid

#### EXPERIMENTAL INVESTIGATION OF THE UNITED STATES NAVY NUMBER 2 STRUT

The precise measurement of the actual drag of bodies shaped for slight resistance is difficult, since the drag is so small compared to the general proportions of the body, and so sensitive to any disturbance or tripping of the surface flow. It is still more difficult to determine experimentally the pressural part of the drag, because it is a small residue of two much larger quantities, viz, the downstream and upstream pressural forces. The frictional part of the drag, being the drag minus its pressural part, is therefore the least precisely determined of the three. For these reasons any experimental measurements of the actual pressure on thick forms of low resistance, however carefully these forms are made and tested, are likely to be more or less unsatisfactory when analyzed.

The basic experimental data for the investigation of the actual flow past the United States Navy Number 2 strut are simply the measurements of the total drag and the point pressures at 14 positions on the strut surface. (Tables VII and VIII.) These data were obtained from a smooth wooden strut model 3 by 10½ by 60 inches faced, where pressures were collected, by a brass plate carefully fitted and perforated by 1-millimeter pressure holes. The ends of the strut were so shielded that the strut was the equivalent of an equal segment of a strut infinitely long. The total drag was measured on the aerodynamic balance, to which the strut was attached by prongs which entered the middle of the strut, as explained in Reference 20. The location of the pressure holes is given in Table VIII. Measurements of drag and pressure were obtained in the large Navy wind tunnel with the air stream held at five different speeds. The laboratory equipment for measuring these quantities and the technique of the experiment will be found clearly discussed in Reference 20, and will not be considered here

Figures 4 and 5, in which the measured pressures are plotted against the strut width and the half thickness, respectively, have already been referred to. In Figure 4 the other four experimental curves are omitted, namely, those for 20, 30, 40, and 50 miles per hour. However, for each speed there is a point of full impact pressure  $q$ , at the nose and two points of zero pressure at the side, the first at a distance of 3.3 per cent of the strut width from the front, and the second at a distance of 87.1 per cent. The corresponding theoretical values are 3.1 per cent for the first, and 92.1 per cent for the second. At about one-fifth of the width from the leading edge occurs the maximum suction which equals about four-fifths of the nose pressure  $q$ . The maximum theoretical suction occurs at the same place but is larger, being about seven-eighths of the nose pressure. At the trailing edge the experimental pressure is about one-sixth  $q$ , while the theoretical pressure there is  $q$ . Throughout most of the suction range the experimental suction is uniformly less than the theoretical by about one-tenth  $q$ . As may be seen from the data, the pressure at each hole varies nearly as the square of the speed, but with a degree of approximation slightly diminishing aft of the thickest part of the strut and more pronouncedly at the lower speeds. That this is even approximately true near the trailing edge indicates that the line of separation moves only slightly, if at all, throughout the speed range covered. This invariance of flow pattern with air speed is also shown by the fact that the rear zero pressure line does not shift along the surface of the strut as the speed is varied. This contrasts with the results obtained on a 2 by 8 inch elliptical cylinder (Reference 20), which has a shifting rear zero-pressure point and a varying flow pattern near the trailing edge.

One must turn to Figure 5 to find the consequence of the variation of the experimental point pressures from the theoretical. In this figure the integrals of the segments of the pressure graphs give the elements of pressural drag and their sum gives the resultant pressural drag. We have already seen that this sum is zero for the theoretical curve. The elements of pressural drag are given both separately and summed for both theory and experiment in Table IX. The lower part of the table is of special interest as showing the relation of the drag to its pressural and frictional parts, and the relation of the pressural drag to its four upstream and downstream parts.<sup>4</sup> At 60 miles per hour air speed, the integral experimental pressures exert an upstream force of 0.6383 pound, and a downstream force of 0.7012 pound per foot of strut length. The resultant pressural drag  $D_p$ , is therefore 0.0629 pound per foot. Since the measured drag at this speed is 0.1748 pound, the frictional drag is 0.1119 pound, being the drag minus its pressural part. The order of graphic integration, used to find the force  $\int p \, dy$  over the various portions of the strut surface, for 1-foot length of strut, is detailed at the bottom of Table IX.

We have just seen that the measured drag exceeds the resultant force of the integrated pressures by 0.1119 pound, and that this is the measured frictional drag. The frictional drag can also be computed from well-known formula for surface friction. Wieselsberger (Reference 19) gives, for example,

$$D_f = C_f O q \quad (26)$$

as the equation for the frictional drag of a plane whose total washed area is  $O$ . In this equation

$$C_f = 0.0375 \left( \frac{v}{LV} \right)^{0.16}$$

where  $L$  is measured along stream, and  $V$  is the stream speed. Writing  $O = 2L$  for 1-foot length of plane, and  $q = \frac{1}{2} \rho V^2$ , equation (26) becomes

$$D_f = 0.0375 \rho v^{0.16} L^{0.85} V^{1.85}$$

or

$$D_f = KL^{0.85} V^{1.85} \quad (27)$$

where  $D_f$  is the frictional drag per foot run and  $K = 0.0375 \rho v^{0.16}$ .

Since one keeps only the downstream component of the tangential friction, the resultant frictional drag over the strut surface is equal, quite approximately, to that over its median plane, when the tangential speeds are the same at equal distances from the leading edge. One

<sup>4</sup> This method is due to Zahm, Reference 17.

has then to apply equation (27) only to the strut median plane, using for  $L$  the distance from the entering edge and for  $V$  the surface speed past the element of strut surface, whose projection on the plane is  $dL$ . From equation (6) the actual surface speed past the strut is  $V = \sqrt{p_0 - p_s}$  where  $p_s$  is the measured pressure and  $U_0 = 1$ . Let  $V = f(L)$  as plotted in Figure 11. Then equation (27) becomes, for  $L$  in feet,

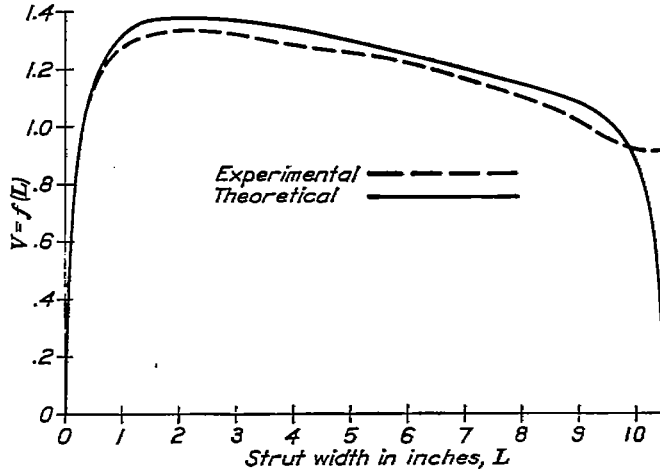


FIGURE 11.—Experimental and theoretical air speeds over surface of United States Navy No. 2 strut for unit stream speed

$$D_f = KL^{0.85}f^{1.85}$$

or

$$dD_f = K[0.85 L^{-0.15}f^{1.85}dL + 1.85L^{0.85}f^{0.85}f'dL] \tag{27}$$

where  $f'$  is the slope of the curve  $V = f(L)$ . Then

$$D_f = K[0.85 \int L^{-0.15}f^{1.85}dL + 1.85 \int L^{0.85}f^{0.85}f'dL]$$

or

$$D_f = K[I_1 + I_2] \tag{28}$$

The integrals  $I_1$  and  $I_2$  were graphically integrated from curves of  $L^{-0.15}f^{1.85}$  versus  $L$  (fig. 12), the data for which is found in Table X. The value of  $I_1$  and  $I_2$  are found to be  $I_1 = 1.343$ ,  $I_2 = -0.2$  and

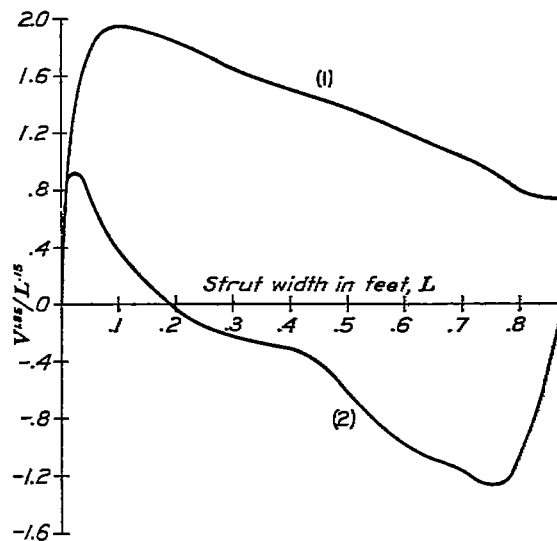


FIGURE 12.—Curves of  $V^{1.85}/L^{0.15}$  versus strut width for unit stream speed. Areas under (1) and (2) give  $I_1$  and  $I_2$  in equation 28

$$I_1 + I_2 = 1.055$$

Since the integration was carried through for a unit stream speed, the total frictional drag at 88 feet per second is

$$D_f = K(1.055) (88^{1.85})$$

Using in  $K$  the values  $\rho = 0.00237$  and  $\nu^{0.15} = 0.2711$ ,

$$D_f = 0.1006.$$

This value compares satisfactorily with

$$D_f = 0.1119$$

found as the excess of total drag over pressural drag, both values being pounds per foot run at 60 miles per hour.

We have found, furthermore, that the measured point pressures and the computed surface friction give, as the value of the total drag of the Navy Number 2 strut, the value

$$D = D_p + D_f = 0.0629 + 0.1006 = 0.1635 \text{ lb./ft.},$$

which is about 6 per cent less than the actual measured drag,

$$D = 0.1748 \text{ lb./ft.}$$

#### CONCLUSIONS

The theoretical flow past symmetrical forms of predetermined shape can be rigorously solved by use of von Karman's adaptation of Rankine's theory, but not yet by Joukowski's theory or any of its extensions.

Using the empirical United States Navy Number 2 strut as the predetermined shape, the pressures about a very close approximation from the Joukowski theory and about the exact form from the Rankine theory agree within the precision of the computations. While agreement between the theories was to be expected, still it is reassuring to have two theoretical treatments, which are so widely different as these in their mathematical premises and developments, to finally give the same results for an actual body, especially since the body, being empirical, allowed no advantage to either.

The frictional resistance, determined from experiment, agrees, for the strut studied, within 10 per cent with that computed from the experimental surface speeds, and would agree still better with that computed from the theoretical surface speeds. Also the total resistance as measured agrees within 6 per cent with that computed from experimental surface pressure and friction. These agreements are rather better than one should expect, considering the fact that some of the quantities are small-order residues, and probably can not be taken as indicating the accuracy of such analyses in general. They tend to show, however, that the parts of the whole drag experienced by a body moving through a real fluid can be fully accounted for and accurately calculated from surface pressure and friction, granting sufficiently accurate experimental measurements of surface pressure.

#### REFERENCES

- Reference 1. Rankine, W. J. M.: On Plane Water Lines in Two Dimensions. Philosophical Transactions, 1864, p. 369.
- Reference 2. Rankine, W. J. M.: On the Mathematical Theory of Streamlines, Especially Those with Four Foci and Upwards. Philosophical Transactions, 1871, p. 267.
- Reference 3. Taylor, D. W.: On Ship-Shaped Stream Forms. Transactions of the British Institute of Naval Architects, 1894.
- Reference 4. Taylor, D. W.: On Solid Stream Forms and the Depth of Water Necessary to Avoid Abnormal Resistance of Ships. Transactions of the British Institute of Naval Architects, 1895.
- Reference 5. McEntee, William: On Some Ship-Shaped Stream Forms. Transactions of the Society of Naval Architects and Marine Engineers, 1909.
- Reference 6. Fuhrmann, G.: Theoretische und Experimentelle Untersuchungen an Balloonmodellen, Jahrbuch der Motorluftschiff-Studien-Gesellschaft, Band V, 1911-12.

- Reference 7. Joukowski, N.: *Aerodynamique*, 1916.
- Reference 8. Mises, R. von: *Zur Theorie des Tragflachen-auftriebes*, *Zeitschrift für Flugtechnik und Motorluftschiffahrt*, Vol. 1917, p. 157, et Vol. 1920, p. 68.
- Reference 9. Betz, A.: *Beiträge zur Tragflügeltheorie, mit besonderer Berücksichtigung des einfachen rechteckigen Flügels*. Diss. Göttingen, 1919.
- Reference 10. Kutta, W. M.: *Über ebene Zirkulationströmungen, nebst flugtechnischen Anwendungen*. Sitzungsberichte der Bayer. Akademie der Wissenschaften, 1910 and 1911.
- Reference 11. Nüller, Wilhelm: *Über der Form- und Auftriebsinvarianten für eine besondere Klasse von Flügelprofilen*, p. 389; and *Zur Konstruktion von Tragflachenprofilen*, p. 213. *Zeitschrift für Angewandte Mathematik und Mechanik*, Band 4, 1924.
- Reference 12. Witoszynski, C.: *On the Motion of Cylinders in a Perfect Fluid*. *Przeglad Techniczny (Technical Review)*, Warsaw, Poland, 1919.
- Reference 13. Warner, Edward P.: *Aerodynamics: Airplane Design*, 1927, p. 214.
- Reference 14. Karman, Th. v.: *Berechnung der Druckverteilung an Luftschiffkörpern*. *Abhandlungen aus dem Aerodynamischen Institut an der Technischen Hochschule, Aachen*, 1927.
- Reference 15. Prandtl, L.: *Applications of Modern Hydrodynamics to Aeronautics*. N. A. C. A. Technical Report No. 116, Washington, 1921.
- Reference 16. Glauert, H.: *Airfoil and Airscrew Theory*, 1926, pp. 115-116.
- Reference 17. Zahm, A. F., Smith, R. H., and Hill, G. C.: *Point Drag and Total Drag of Navy Struts No. 1 Modified*. N. A. C. A. Technical Report No. 137, Washington, 1922.
- Reference 18. Zahm, A. F.: *Flow and Drag Formulas for Simple Quadrics*. N. A. C. A. Technical Report No. 253, Washington, 1927.
- Reference 19. Wieselsberger, C.: *Ergebnisse der Aerodynamischen Versuchsanstalt zu Göttingen*, 1 Lieferung 1921, p. 120.
- Reference 20. Zahm, A. F., Smith, R. H., and Loudon, F. A.: *Forces on Elliptic Cylinders in Uniform Air Stream*. N. A. C. A. Technical Report No. 289, 1928.
- Reference 21. Wieselsberger, C.: *Linien Konstanter Strömungsgeschwindigkeit*, Report of the Aeronautical Research Institute, Tokyo Imperial University, Vol. II.

AERODYNAMICAL LABORATORY,  
BUREAU OF CONSTRUCTION AND REPAIR,  
NAVY YARD, *Washington, D. C.*

TABLE I  
 Constants  $\varphi_{Lp}$  in Equations 1 and 2

1	2	3	4	5	6	7	8	9	10	11	12	13	$2rUy$
+	+	+	+	+	+	+	+	+	+	+	+	+	+
1.000	1.000	1.000	1.000	1.000	1.000	1.000	1.000	1.000	1.000	1.000	1.000	1.000	0
+	+	+	+	+	+	+	+	+	+	+	+	+	+
1.571	1.039	.7045	.4520	.2761	.1684	.0969	.0666	.0507	.0409	.0373	.0343	.0335	4.273
+	+	+	+	+	+	+	+	+	+	+	+	+	+
1.893	1.571	1.249	.8761	.5405	.3217	.1801	.1219	.0921	.0740	.0674	.0619	.0603	7.540
+	+	+	+	+	+	+	+	+	+	+	+	+	+
2.047	1.823	1.571	1.201	.7703	.4516	.2446	.1635	.1225	.0980	.0891	.0816	.0793	9.739
+	+	+	+	+	+	+	+	+	+	+	+	+	+
2.201	2.051	1.873	1.571	1.090	.6350	.3302	.2147	.1588	.1257	.1137	.1038	.1012	12.064
+	+	+	+	+	+	+	+	+	+	+	+	+	+
2.364	2.274	2.167	1.972	1.571	.9750	.4741	.2938	.2113	.1646	.1481	.1347	.1311	14.828
+	+	+	+	+	+	+	+	+	+	+	+	+	+
2.539	2.489	2.432	2.328	2.098	1.571	.7423	.4177	.2845	.2148	.1914	.1722	.1671	17.279
+	+	+	+	+	+	+	+	+	+	+	+	+	+
2.737	2.715	2.691	2.649	2.564	2.356	1.571	.7534	.4384	.3031	.2618	.2301	.2218	18.849
+	+	+	+	+	+	+	+	+	+	+	+	+	+
2.863	2.852	2.840	2.821	2.783	2.701	2.401	1.571	.7400	.4282	.3502	.2955	.2814	18.347
+	+	+	+	+	+	+	+	+	+	+	+	+	+
2.963	2.957	2.952	2.942	2.925	2.890	2.780	2.494	1.571	.6478	.4672	.3616	.3373	15.205
+	+	+	+	+	+	+	+	+	+	+	+	+	+
3.039	3.037	3.034	3.030	3.022	3.007	2.967	2.882	2.653	1.571	.8153	.4885	.4307	10.681
+	+	+	+	+	+	+	+	+	+	+	+	+	+
3.076	3.074	3.072	3.070	3.066	3.057	3.035	2.993	2.897	2.498	1.571	.6434	.5191	7.540
+	+	+	+	+	+	+	+	+	+	+	+	+	+
3.113	3.112	3.112	3.111	3.109	3.106	3.097	3.082	3.053	2.965	2.799	1.571	.8506	3.581

TABLE II

Pressure and velocity over the separation surface whose form is the Navy No. 2 strut

Point p	x	y	$U_x$	$v_x$	$(1+u_x)^2$	$v_x^2$	$q_x^2$	$p=1-q_x^2$
0	0	0	-1.000	0	0	0	0	+1.000
1	.200	.680	-.634	+.488	+.134	+.238	+.372	+.628
2	.600	1.200	-.317	+.724	+.466	+.524	+.990	+.010
3	1.000	1.251	-.069	+.680	+.868	+.462	+1.330	-.330
4	1.600	1.918	+.126	+.588	+1.264	+.346	+1.610	-.610
5	2.600	2.360	+.279	+.452	+1.636	+.204	+1.840	-.840
6	4.200	2.751	+.356	+.211	+1.839	+.044	+1.883	-.883
7	7.200	3.000	+.331	+.045	+1.772	+.002	+1.774	-.774
8	10.400	2.920	+.279	-.116	+1.636	+.013	+1.650	-.450
9	13.600	2.418	+.178	-.272	+1.388	+.074	+1.462	-.462
10	16.800	1.700	+.109	-.243	+1.230	+.059	+1.289	-.289
11	18.400	1.202	-.044	-.468	+.913	+.219	+1.132	-.132
12	20.000	.570	-.128	-.098	+.760	+.010	+.770	+.230

TABLE III

The x and y coordinates of the Joukowski strut, transformed from the circle  $a=2.00$  centered at  $\xi=-0.20$ , by equations 10, when the map circle is  $b=1.48$

Point p	Round cylinder		Joukowski strut		Navy No. 2 strut		Per cent of maximum y error in y
	$\xi$	$\eta$	x	y	x	y	
0	-2.200	0	-3.196	0	-3.196	0	0
1	-2.170	+.347	-3.154	+.190	-3.154	+.186	+.4
2	-2.079	+.684	-3.030	+.371	-3.030	+.361	+.9
3	-1.932	+1.000	-2.826	+.535	-2.826	+.529	+.6
4	-1.732	+1.286	-2.547	+.680	-2.547	+.680	0
5	-1.486	+1.532	-2.200	+.795	-2.200	+.793	+.2
6	-1.200	+1.732	-1.792	+.877	-1.792	+.877	0
7	-.719	+1.932	-1.089	+.936	-1.089	+.936	0
8	-.200	+2.000	+.308	+.916	-.308	+.922	-.6
9	+.319	+1.932	+.501	+.827	+.501	+.835	-.9
10	+.800	+1.732	+1.281	+.690	+1.281	+.701	-1.2
11	+1.086	+1.532	+1.760	+.582	+1.760	+.594	-1.4
12	+1.332	+1.286	+2.183	+.464	+2.183	+.476	-1.3
13	+1.532	+1.000	+2.534	+.345	+2.534	+.357	-1.3
14	+1.679	+.684	+2.798	+.228	+2.798	+.258	-3.2
15	+1.800	0	+3.017	0	+3.017	+.175	-18.7

TABLE IV

Values of  $q_r$ ,  $p_r$ ,  $r$ ,  $\theta$  from equation 22 giving surfaces of constant speed near the round cylinder, from  $q_r=0.250$  to  $q_r=1.000$ , omitting  $q_r=1.118$  to  $q_r=1.750$

$q_r$	$p_r$	r	$\theta$	$q_r$	$p_r$	r	$\theta$
0.250	0.937	2.00	7 11	0.707	0.500	2.00	20 50
		2.05	7 15			2.25	23 20
		2.10	6 59			2.50	23 10
		2.15	6 31			2.75	23 20
		2.20	5 43			3.00	19 20
		2.25	4 26			3.25	17 10
		2.30	1 44			3.50	13 50
		2.31	0			4.00	0
.500	.750	2.00	14 29	.866	.250	2.00	25 40
		2.10	15 2			2.25	28 10
		2.20	14 49			2.50	29 30
		2.30	14 31			2.75	31 30
		2.40	13 39			3.00	31 20
		2.50	12 31			3.25	31 20
		2.70	8 23			3.50	35 20
		2.83	0			4.00	26 50
.750	.438	2.00	22 2	1.000	0	2.00	30 0
		2.25	23 55			2.50	35 40
		2.50	24 17			3.00	38 35
		2.75	23 41			3.50	40 18
		3.00	22 12			4.00	41 24
		3.25	20 7			5.00	42 42
		3.50	16 46			6.00	43 24
		4.00	0			8.00	44 6

TABLE V-a

Contour, velocity, and pressure values for the round cylinder  $a=2.00$  centered at  $\xi=-0.20$  and for the corresponding Joukowski strut when map cylinder is  $b=1.48$

$\psi$	Round cylinder					Joukowski strut				
	$\eta$	$\xi$	$u_r$	$v_r$	$q_r$	$x$	$y$	$ \frac{dz}{d\zeta} $	$q_s$	$p_s$
Eq. 25			Eq. 14, 15, 18			Eq. 10		Eq. 17	Eq. 16	Eq. 6
0	0	-4.200	+0.750	0	0.750	-4.721	0	0.876	0.856	+0.267
0	0	-3.200	+ .556	0	.556	-3.884	0	.786	.707	+ .500
0	0	-2.200	0	0	0	-3.196	0	.547	0	+1.000
0	.347	-2.170	+ .060	+ .342	.347	-3.154	+ .190	.586	.592	+ .650
0	.684	-2.079	+ .234	+ .643	.684	-3.030	+ .371	.688	.994	+ .012
0	1.000	-1.932	+ .500	+ .860	1.000	-2.826	+ .537	.824	1.213	- .472
0	1.286	-1.732	+ .826	+ .985	1.286	-2.547	+ .680	.974	1.320	- .741
0	1.532	-1.486	+1.173	+ .985	1.532	-2.200	+ .795	1.122	1.366	- .865
0	1.732	-1.200	+1.500	+ .877	1.732	-1.792	+ .877	1.261	1.374	- .867
0	1.932	- .719	+1.866	+ .501	1.932	-1.090	+ .936	1.429	1.351	- .719
0	2.000	- .200	+2.000	0	2.000	- .308	+ .916	1.535	1.303	- .697
0	1.932	+ .319	+1.866	- .501	1.932	+ .501	+ .827	1.552	1.245	- .549
0	1.732	+ .800	+1.500	- .867	1.732	+1.281	+ .690	1.464	1.183	- .401
0	1.532	+1.086	+1.173	- .985	1.532	+1.760	+ .580	1.341	1.142	- .305
0	1.286	+1.332	+ .826	- .985	1.286	+2.183	+ .464	1.168	1.101	- .212
0	1.000	+1.532	+ .500	- .867	1.000	+2.535	+ .346	.949	1.053	- .110
0	.684	+1.679	+ .234	- .643	.684	+2.798	+ .228	.700	.976	+ .046
0	0	+1.800	0	0	0	+3.017	0	.324	0	+1.000
0	0	+2.800	+ .556	0	.556	+3.582	0	.721	.771	+ .405
0	0	+3.800	+ .750	0	.750	+4.376	0	.848	.884	+ .218

TABLE V-b

Contour, velocity, and pressure values for closely graded streamlines,  $\psi=const.$  used to find constant speed surfaces near strut.  $\psi=0.03, 0.05, 0.10, 0.20, 0.50$  omitted

$\psi$	Round cylinder					Joukowski strut				
	$\eta$	$\xi$	$u_r$	$v_r$	$q_r$	$x$	$y$	$ \frac{dz}{d\zeta} $	$q_s$	$p_s$
Eq. 25			Eq. 14, 15, 18			Eq. 10		Eq. 17	Eq. 16	Eq. 6
0.01	0.05	+2.155	+0.280	+0.031	0.281	+3.171	+0.026	0.530	0.531	+0.718
.01	.05	-2.555	+ .280	- .031	.281	-3.412	+ .033	.512	.550	+ .698
.01	.10	+1.903	+ .102	+ .086	.133	+3.051	+ .040	.405	.329	+ .892
.01	.10	-2.303	+ .102	- .086	.133	-3.283	+ .059	.591	.225	+ .949
.01	.15	+1.865	+ .076	+ .135	.155	+3.032	+ .056	.395	.392	+ .846
.01	.15	-2.265	+ .076	- .135	.155	-3.228	+ .086	.581	.267	+ .929
.01	.20	+1.821	+ .049	+ .190	.196	+3.010	+ .104	.390	.503	+ .746
.01	.20	-2.221	+ .049	- .190	.196	-3.199	+ .168	.572	.343	+ .882
.01	.40	+1.786	+ .101	+ .377	.390	+2.933	+ .143	.498	.784	+ .386
.01	.40	-2.186	+ .101	- .377	.390	-3.155	+ .222	.606	.645	+ .534
.01	.70	+1.689	+ .253	+ .642	.690	+2.796	+ .241	.709	.972	+ .054
.01	.70	-2.089	+ .253	- .642	.690	-3.032	+ .384	.695	.992	+ .016
.01	1.00	+1.544	+ .500	+ .844	.971	+2.543	+ .352	.943	1.029	- .059
.01	1.00	-1.944	+ .500	- .844	.971	-2.835	+ .541	.823	1.180	- .392
.01	1.50	+1.133	+1.117	+ .986	1.490	+1.835	+ .570	1.313	1.135	- .288
.01	1.50	-1.533	+1.117	- .986	1.490	-2.263	+ .786	1.098	1.357	- .842
.01	2.00	- .060	+1.985	+1.390	1.982	+ .092	+ .906	1.546	1.282	- .643
.01	2.00	- .340	+1.985	-1.390	1.982	- .521	+ .936	1.493	1.328	- .763

TABLE V-c

Contour, velocity, and pressure values for normally graded streamlines,  $\psi = \text{const.}$   $\psi = 0.70, 1.05, 1.40, 1.75, 2.10,$  and  $2.45$  omitted

$\psi$	Round cylinder					Joukowski strut				
	$x$	$y$	$u_x$	$u_y$	$u_z$	$x$	$y$	$\left \frac{dz}{dz'}\right $	$q_x$	$p_x$
	Eq. 25		Eq. 14, 15, 18			Eq. 10		Eq. 17	Eq. 16	Eq. 6
0.35	0.35	+	1.000	0	1.000	+	+0.350	0	1.000	0
.35	.35	-	1.000	0	1.000	-	+0.350	0	1.000	0
.35	.50	+3.417	+0.711	+0.081	.716	+4.044	+0.403	.826	.867	+0.248
.35	.50	-3.817	+0.711	-0.081	.716	-4.381	+0.426	.858	.834	+0.304
.35	.70	+2.540	+0.561	+0.240	.610	+3.342	+0.479	.732	.834	+0.304
.35	.70	-2.940	+0.561	-0.240	.610	-3.645	+0.532	.786	.777	+0.397
.35	.80	+2.344	+0.539	+0.232	.611	+3.181	+0.514	.750	.815	+0.335
.35	.80	-2.744	+0.539	-0.232	.611	-3.480	+0.585	.787	.777	+0.396
.35	1.00	+2.070	+0.561	+0.479	.731	+2.928	+0.586	.810	.903	+0.185
.35	1.00	-2.470	+0.561	-0.479	.731	-3.232	+0.692	.807	.906	+0.179
.35	1.25	+1.798	+0.685	+0.647	.937	+2.619	+0.679	.933	.993	+0.013
.35	1.25	-2.198	+0.685	-0.647	.937	-2.951	+0.823	.876	1.071	-0.145
.35	1.50	+1.523	+0.894	+0.759	1.173	+2.253	+0.781	1.102	1.064	-0.133
.35	1.50	-1.923	+0.894	-0.759	1.173	-2.631	+0.947	.963	1.218	-0.433
.35	1.75	+1.192	+1.180	+0.779	1.411	+1.774	+0.895	1.263	1.116	-0.246
.35	1.75	-1.592	+1.180	-0.779	1.411	-2.215	+1.065	1.093	1.290	-0.665
.35	2.00	+0.721	+1.536	+0.627	1.659	+1.070	+1.031	1.407	1.179	-0.390
.35	2.00	-1.121	+1.536	-0.627	1.659	-1.588	+1.167	1.268	1.308	-0.712
.35	2.10	+0.424	+1.698	+0.455	1.758	+0.627	+1.098	1.452	1.211	-0.466
.35	2.10	-0.824	+1.698	-0.455	1.758	-1.179	+1.196	1.347	1.304	-0.702

TABLE VI-a

Constant speed contours about the Joukowski strut

$\psi$	$p$	Bow		Stern		$\psi$	$p$	Aft	
		$x$	$y$	$x$	$y$			$x$	$y$
0.25	+0.937	-3.188	0.075	+3.012	0.013	1.25	-0.563	-2.800	0.570
		-3.237	.077	+3.050	0			-2.750	.600
.25	+0.937	-3.315	.050					-2.700	.660
		-3.330	0					-2.640	.730
.50	+0.75	See Table VI-b						-2.550	.830
.75	+0.438	-3.125	0.250	+2.960	0.125			-2.380	1.015
		-3.158	.315	+3.025	.300			-2.152	1.180
		-3.200	.362	+3.125	.340			-1.600	1.330
		-3.300	.450	+3.340	.300			-1.165	1.175
		-3.470	.520	+3.520	.065			+0.050	1.070
		-3.670	.520	+3.525	0			+0.270	.935
		-3.890	.412			1.25	-0.563	+0.375	.870
		-4.000	.250					+0.412	.835
		-4.040	.140						
.75	+0.438	-4.050	0						
1.00	0	-3.025	.380	+2.750	.250				
		-3.025	.440	+2.680	.350				
		-3.030	.510	+2.637	.440				
		-3.048	.610	+2.600	.525				
		-3.080	.775	+2.570	.692				
		-3.130	.910	+2.550	.845				
		-3.200	1.080	+2.570	1.048				
		-3.360	1.400	+2.660	1.375				
		-3.535	1.730	+2.800	1.720				
1.00	0	-3.730	2.052	+2.975	2.030				

TABLE VI-b

Constant pressure contours about Joukowski strut

p	q	Bow		Stern		p	q	Aboard	
		x	y	x	y			x	y
+0.75	0.50	-3.175	0.160	+3.008	0.030	-0.25	1.118	-2.940	0.451
		-3.180	.170	+3.033	.060			-2.900	.625
		-3.260	.210	+3.108	.065			-2.730	.880
+.75	.50	-3.470	.130	+3.135	.030			-2.790	1.020
		-3.525	0	+3.150	0			-2.725	1.240
+.50	.707	-3.130	.240	+2.975	.095			-2.600	1.600
		-3.170	.290	+3.000	.170			+1.975	.527
		-3.230	.330	+3.050	.235			+1.830	.750
		-3.330	.375	+3.350	.175			+1.745	.900
		-3.775	.290	+3.395	.075			+1.660	1.030
		-3.830	.140	+3.410	0			+1.210	1.635
+.50	.707	-3.900	.050			-.25	1.118	-2.825	.535
		-3.900	0					-2.700	.700
+.25	.866	-3.085	.310	+2.900	.175			-2.480	1.000
		-3.105	.370	+2.913	.250			-2.080	1.370
		-3.130	.425	+2.930	.330			-2.240	1.480
		-3.190	.525	+2.965	.400			+1.135	1.260
		-3.295	.652	+3.045	.535			+1.330	1.120
		-3.490	.800	+3.375	.670			+1.750	.790
+.25	.866	-3.950	.900	+3.820	.613	-.50	1.225	-2.500	.696
		-4.310	.851	+4.180	0			-2.320	.880
		-4.700	.580					-2.000	.975
		-4.775	.420					-2.230	1.075
+.25	.866	-4.820	0					-1.820	1.025
0	1.00	See Table VI-a				-0.75	1.323	-1.565	.930

TABLE VII

Resistance values for Navy No. 2, 5-foot strut with shielded ends at various air speeds and zero pitch and yaw

Air-speed, M.P.H. V	Net resist- ance per foot R lb.	$V_1 D_1$ (ft. x ft./sec.)	$C = \frac{Rg}{\rho L D_1 V^3}$
20	0.0240	7.34	0.0940
30	.0472	11.00	.0821
40	.0796	14.67	.0779
50	.1206	18.34	.0755
60	.1748	22.00	.0761

R=resistance per foot length of strut, lb.  
D=strut thickness in inches.  
D<sub>1</sub>=strut thickness in feet.  
C=shape coefficient.  
V=air speed in miles per hour.  
V<sub>1</sub>=air speed in feet per second.  
ρ/g=0.00237 slug/feet.

TABLE VIII

Point pressure in terms of nose pressure,  $p/p_n$ , at various wind speeds for Navy No. 2 strut—zero of pitch and yaw

Number	Pressure hole		Point pressure $p/p_n$				
	Coordinates		Wind speed in M. P. H.				
	$x$	$y$	20	30	40	50	60
1	0	0	+1.000	+0.998	+1.004	+1.000	+1.000
2	.100	.370	+ .608	+ .602	+ .601	+ .604	+ .600
3	.320	.620	+ .066	+ .066	+ .071	+ .068	+ .066
4	.540	.830	- .332	- .348	- .345	- .350	- .356
5	.880	1.000	- .612	- .608	- .593	- .604	- .594
6	1.300	1.170	- .704	- .712	- .695	- .706	- .700
7	2.100	1.370	- .780	- .784	- .762	- .768	- .766
8	3.640	1.500	- .688	- .698	- .667	- .668	- .662
9	5.250	1.460	- .586	- .586	- .570	- .566	- .552
10	6.800	1.210	- .414	- .408	- .386	- .386	- .380
11	8.400	.850	- .178	- .176	- .158	- .152	- .146
12	9.220	.590	- .026	- .010	+ .016	+ .022	+ .042
13	9.950	.300	+ .142	+ .154	+ .153	+ .150	+ .146
14	10.330	.100	+ .178	+ .172	+ .170	+ .168	+ .162

$p$  = point pressure at any hole.  
 $p_n$  = point pressure at nose =  $\frac{1}{2}\rho U_\infty^2$

TABLE IX

Along-stream forces per foot run of Navy No. 2 strut expressed both in pounds and in per cent of total drag for theory and experiment at 60 miles per hour

Air speed M. P. H.	Downstream			Upstream			Pressure drag $D_p = P_1 - P_2$	Friction drag $D_f$	Total drag $D = D_p + D_f$
	Push	Suction	Total $P_1$	Push	Suction	Total $P_2$			
Pounds per foot run—theory									
60	0.4151	0.4109	0.8260	0.2010	0.6250	0.8260	0	0	0
Pounds per foot run—experiment									
60	0.4230	0.2752	0.7012	0.0893	0.5490	0.6383	0.0629	0.1119	0.1748
Per cent of total drag—experiment									
60	242	159	401	51	314	365	36	64	100

DIAGRAM I

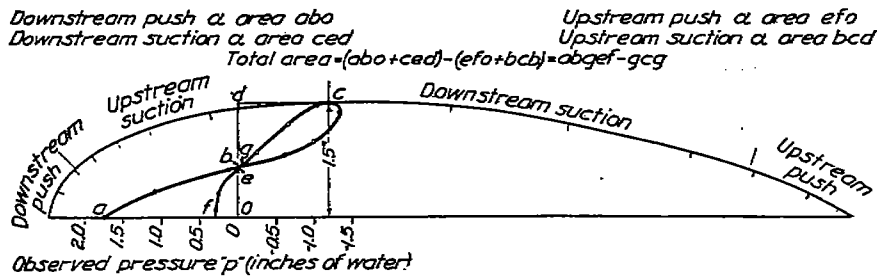


TABLE X

Values of abscissæ, air speeds, and accelerations used in evaluating  $I_1$  and  $I_2$  in Equation 18

Distance aft bow $Z$ in feet	Measured tangential speed $V_s$	$V_{s,0.55} = f_{0.55}$	$V_{s,1.45} = f_{1.45}$	$L_{0.55}$	$L_{1.45} = L_{0.55}$	$\frac{dV_s}{dL} = f'$ (ft/sec)	$\frac{1.85 \times}{f_{0.55} L_{0.55}^2} =$ $I_1$	$\frac{0.85 \times}{f_{1.45} L_{1.45}^2} =$ $I_2$
0	0	0	0	0	0			
.0208	.920	.930	.855	.0373	1.793	+14.40	+0.924	+1.303
.0417	1.125	1.105	1.243	.0671	1.809	+6.288	+ .862	+1.700
.0833	1.276	1.233	1.573	.1210	1.453	+1.675	+ .462	+1.943
.1250	1.316	1.262	1.661	.1708	1.366	+ .624	+ .249	+1.930
.1666	1.330	1.274	1.695	.2181	1.309	+ .156	+ .080	+1.886
.2083	1.330	1.274	1.695	.2635	1.263	- .108	- .067	+1.820
.2500	1.318	1.265	1.666	.3079	1.232	- .222	- .160	+1.744
.2916	1.298	1.248	1.621	.3506	1.203	- .270	- .219	+1.657
.3333	1.282	1.235	1.584	.3932	1.179	- .292	- .262	+1.587
.3748	1.268	1.224	1.552	.4345	1.158	- .294	- .289	+1.528
.4166	1.256	1.214	1.524	.4749	1.139	- .320	- .341	+1.475
.4585	1.242	1.203	1.493	.5152	1.123	- .387	- .444	+1.425
.5000	1.220	1.184	1.444	.5546	1.113	- .511	- .621	+1.366
.5415	1.194	1.163	1.388	.5930	1.094	- .622	- .794	+1.291
.5832	1.165	1.139	1.326	.6321	1.084	- .711	- .947	+1.222
.6250	1.135	1.113	1.264	.6693	1.071	- .765	-1.087	+1.151
.6666	1.102	1.086	1.197	.7083	1.062	- .788	-1.122	+1.081
.7082	1.067	1.057	1.127	.7460	1.052	- .826	-1.205	+1.008
.7500	1.016	1.014	1.030	.7828	1.043	- .871	-1.279	+1.913
.7915	.956	.961	.918	.8185	1.034	- .780	-1.133	+ .807
.8333	.920	.930	.855	.8566	1.028	- .474	- .698	+ .747
.8755	.916	.929	.850	.8930	1.020	- .030	- .046	+ .737